A 3-D Meshfree Numerical Model to Analyze Cellular Scale Shrinkage of Different Categories of Fruits and Vegetables during Drying

†*C.M. Rathnayaka Mudiyanselage [1, 2], H.C.P. Karunasena [3], Y.T. Gu [1], L. Guan [1], J. Banks [1] and W. Senadeera [1]

[1]Queensland University of Technology (QUT), Science and Engineering Faculty, School of Chemistry Physics and Mechanical Engineering, 2-George Street, Brisbane, QLD 4001, Australia.
[2]Department of Chemical and Process Engineering, Faculty of Engineering, University of Moratuwa, Moratuwa, Sri Lanka.
[3]Department of Mechanical and Manufacturing Engineering, Faculty of Engineering, University of Ruhuna, Hapugala, Galle, Sri Lanka.

*Presenting author: charith.rathnayaka@hdr.qut.edu.au
†Corresponding author: charith.rathnayaka@hdr.qut.edu.au

Abstract

In order to optimize food drying operations, a good understanding on the related transport phenomena in food cellular structure is necessary. With that intention, a three-dimensional (3-D) numerical model was developed to better investigate the morphological changes and related solid and fluid dynamics of single parenchyma cells of apple, carrot and grape during drying. This numerical model was developed by coupling a meshfree particle based method: Smoothed Particle Hydrodynamics (SPH) with a Discrete Element Method (DEM). Compared to conventional grid-based numerical modelling techniques such as Finite Element Methods (FEM) and Finite Difference Methods (FDM), the proposed model can better simulate deformations and cellular shrinkage within a wide range of moisture content reduction. The model consists of two main components: cell fluid and cell wall. The cell fluid model is based on SPH and represents the cell protoplasm as a homogeneous Newtonian liquid. The cell wall model is based on a DEM and approximates the cell wall to an incompressible Neo-Hookean solid material. A series of simulations were conducted to mimic the gradual shrinkage during drying as a function of moisture content.

Keywords: Food drying; Meshfree methods; Plant cell modelling; Smoothed Particle Hydrodynamics (SPH); Three-dimensional (3-D) model

Introduction

Drying is one of the most common and cost effective techniques for extending the shelf life of food materials and also is used for the production of numerous traditional and innovative food products [1]. It is employed to preserve approximately 20% of the planet's fruits and vegetables [2]. During drying, the moisture is removed out of food material in order to slow down biological activities. With the removal of moisture, the food cellular structure undergoes major structural deformations which influence the drying process performance, food quality and the final market value. Therefore, to develop effective and efficient food drying operations, it is important that these cellular structural deformations are well understood and optimised. In doing so, a thorough understanding of the underlying solid and fluid dynamics is pivotal. The key driving forces for the transport phenomena are the moisture content [3-8] and the drying temperature [9]. The moisture content has a strong relationship with the cell turgor pressure [10] and the drying temperature links with the relative humidity and the rate at which moisture is removed from the cellular structure during

drying. To derive appropriate relationships among such driving forces, cellular morphogenesis and underlying transport phenomena, various microscale theoretical [11, 12] and empirical [3, 5, 13] models have been developed.

Numerical modelling has been utilised as an efficient tool in the studies of deformational analysis of various materials. Until recent times, this had not been used for comprehensive analysis of micro-structural deformations of food materials during drying. However, numerical modelling has recently attracted much attention as a viable tool for this purpose [14-16]. It is believed that through an accomplished numerical model, vast benefits could be obtained in food engineering in terms of drying process performance and predicting the final quality of the dried food product. With this background, this study aimed to develop a three-dimensional (3-D) numerical model in order to investigate the morphological changes and related solid and fluid dynamics of parenchyma cells of apple, carrot and grape during drying. For the implementation, more versatile and novel meshfree particle methods have been chosen over the classical grid-based methods. A series of simulations were conducted to predict the shrinkage of each food tissue variety as a function of the moisture content.

Methodology

3-D Representation of a Single Cell

For this study, a single cell of a cortex (parenchyma) tissue is considered, which is the fundamental building block of most bulk plant tissue structures. This type of a cell could be physically regarded as a stiff and thin-walled vessel containing a viscous fluid. Therefore, the developed numerical model is composed of two main components: cell wall and cell fluid. Based on the literature, the basic geometrical shape of a single cell was assumed to be spherical (see Figure 1) [17]. In the cell fluid model, the fluid volume was approximated to a sphere and the cell wall was approximated to a hollow 3-D spherical shell, enclosing the fluid sphere. The cell fluid hydrodynamic pressure is counterbalanced by the tension of the cell wall. Cell fluid was assumed to be incompressible and the system as a whole was treated as an isothermal unit.

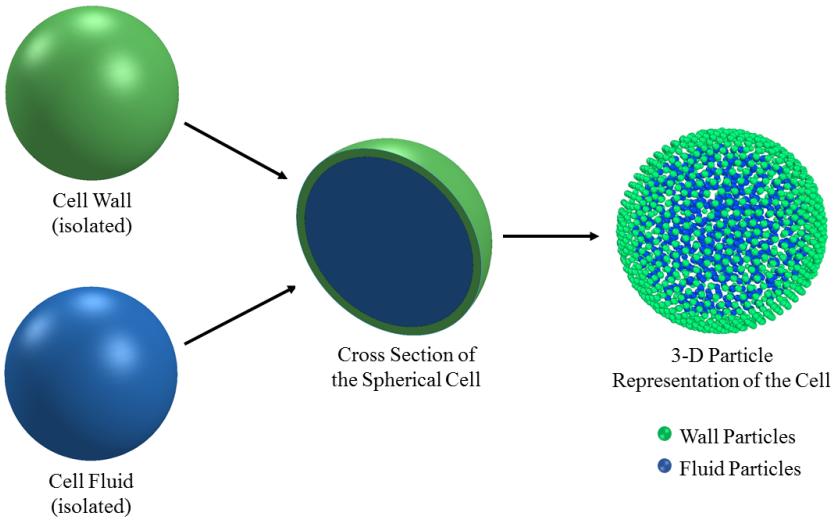

Figure 1. 3-D particle representation of the cell model, which is composed of two sub-models: cell fluid model and cell wall model

After establishing these fundamental assumptions, the cell fluid and cell wall were separately discretised into particle schemes. The intention of this discretisation was to represent the whole system using a large number of non-interconnected particles in order to satisfy the fundamentals of Meshfree Particle Methods (e.g. Smoothed Particle Hydrodynamics (SPH) [18]). Due to the adaptivity and flexibility of the adopted particle framework, it could be easily extended up to multiple cell systems by aggregating more cells together [19, 20]. At the same time, it has the capability to analyse different types of cells (apple, carrot etc.) without significant changes in the main modelling and simulation framework [21]. Furthermore, this particular modelling technique also ensures the ability to incorporate the mechanisms at the subcellular level.

Cell Fluid Model

protoplasm, which can be about 80-90% by volume [22], the cell fluid was approximated to an incompressible homogeneous Newtonian fluid equivalent to water with an elevated viscosity. This can be effectively modelled with Smoothed Particle Hydrodynamics (SPH) considering low Reynolds number flow characteristics [19, 23-25]. Accordingly, in order to model the cell fluid, four different types of forces were used: pressure forces (F^p), viscous forces (F^v), wall-fluid repulsion forces (F^{rw}) and wall-fluid attraction forces (F^a) as presented in Figure 2 [14, 26, 27]. The cumulative effect of these forces is used to define the total force (F_i) on any fluid particle i as,

$$\boldsymbol{F}_i = \boldsymbol{F}^{p}_{ii'} + \boldsymbol{F}^{v}_{ii'} + \boldsymbol{F}^{rw}_{ik} + \boldsymbol{F}^{a}_{ik} \,. \tag{1}$$

Where i' represents the neighboring fluid particles and k the interacting wall particles

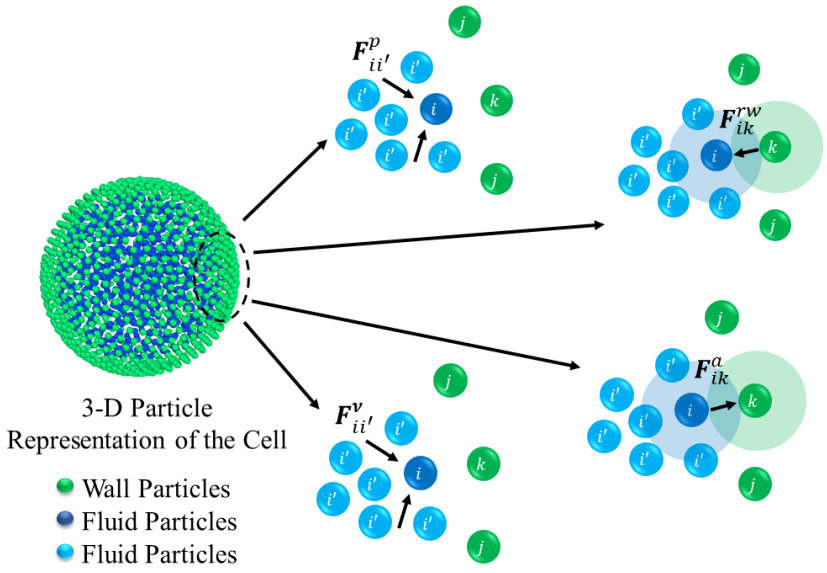

Figure 2. Force fields on the 3-D fluid particle domain: pressure forces (F^p), viscous forces (F^v), wall-fluid repulsion forces (F^{rw}) and wall-fluid attraction forces (F^a)

Cell Wall Model

The cell wall was approximated to a Neo-Hookean solid material. It has been treated as a particle scheme composed of interconnected discrete elements connected to each other via a network, such that each element carries properties of the corresponding cell wall element. The cell wall deformations are represented by the displacement of respective particles under four types of force interactions: stiff forces (F^e), damping forces (F^d), wall-fluid repulsion forces (F^{rf}) and wall-fluid attraction forces (F^a), as illustrated in Figure 3. [14, 15, 26]. Accordingly, the total force (F_k) on any wall particle k is derived as,

$$F_k = F^e_{kj} + F^d_{kj} + F^{rf}_{ki} + F^a_{ki}\,, \tag{2}$$

Where, for each wall particle *k*, *i* indicate the neighboring fluid particles, *j* the bonded wall particles and *l* the non-bonded wall particles

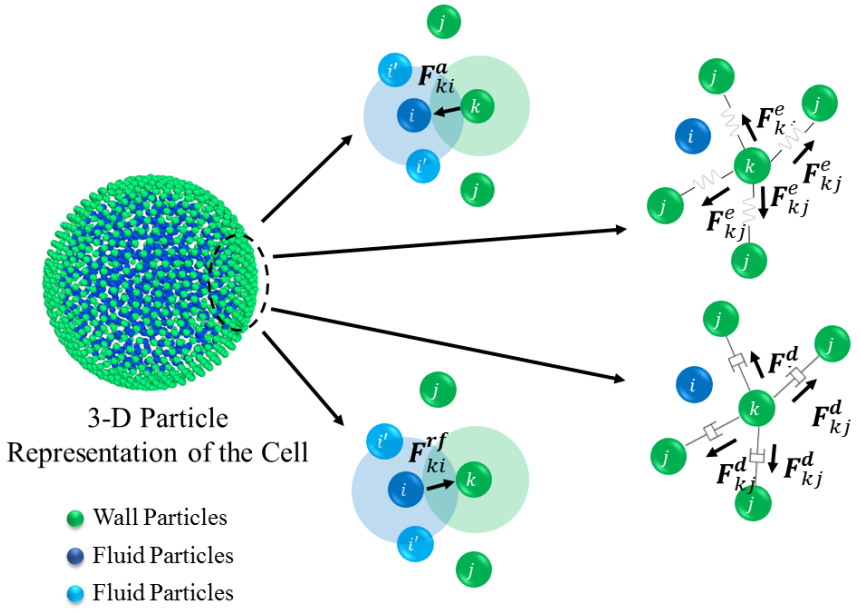

Figure 3. Force fields on the 3-D wall particle domain: stiff forces (F^e), damping forces (F^d), wall-fluid repulsion forces (F^{rf}) and wall-fluid attraction forces (F^a)

Modelling of Different Categories of Fruits and Vegetables

In this study, individual cells of apple, carrot and grape have been modelled. Each food plant material is modelled via customized model parameters obtained from microscopic experimental observations and other numerical models available in the literature. The physical properties necessary for modelling apple, carrot, and grape cells were directly extracted from sources in literature. There were a few properties which had to be calculated and assumed in the process. For instance, shear moduli (G) of the cell wall for carrot and grape were set so that the Young's modulus (E) was 100 MPa which resulted in comparable values for cell wall stiffness at relevant cell wall thickness values. Turgor pressure of grape cells were set equal to the value of apple cells due to the lack of necessary information in literature. This approach has been proven to be successful in similar studies [21]. These

model parameters are outlined in Table 1. The parameters which were used in common for all four plant food categories are shown in Table 2.

Modelling Different Dryness States

The previously mentioned model features were numerically set up with the physical properties of the cells as given in Table 1 and 2. The software tool, COMSOL Multiphysics (COMSOL) was used to generate the initial 3-D particle arrangement in a 3-D sphere corresponding to both the cell fluid and cell wall. There is the possibility to define and fine-tune the initial particle gap and the cell geometrical characteristics using COMSOL in order to obtain the initial particle positions with the preferred and effective particle resolution. The fluid particle scheme was placed without any interconnections among particles, adhering to the SPH fundamentals. In the cell wall, a series of spring networks joining the cell wall particles were used according to the fundamentals of DEM [14, 15, 20] .

It should be noted here that the simulations were carried out mainly based on the moisture content domain, similar to the recent 2-D meshfree based dried plant cell and tissue models [14]. It has also been assumed that the cell turgor pressure stays positive during the entire drying process and it would reduce at a regular rate with the moisture content variation. At the same time, the osmotic potential values corresponding to each dryness states were set equal to the minus value of the relevant turgor pressure and in the meantime the the magnitudes were kept constant in order to assure the stability of the numerical scheme [21].

Table 1. Values of the physical parameters adopted in the model

Parameter	Food variety used for modelling		
	Apple	Carrot	Grape
Initial cell diameter (D_0) (μm)	150	100	150
Cell wall thickness (T_0) (nm)	126	126	62
Wall shear modulus (G) (MPa)	18	33	33
Fresh cell turgor pressure (P_T) (kPa)	200	400	200
Fresh cell osmotic potential (π_T) (kPa)	-200	-400	-200

As the model evolves with time according to the difference between the cell turgor pressure and the osmotic potential, the mass of the cell fluid tends to change and causing slight density variations [14, 15]. Such changes of density cause significant changes in cell turgor pressure as governed by an equation of state (EOS). These turgor pressure variations tend to push the cell wall inwards (shrinkage) or outwards (inflation) causing the cell volume, equivalent diameter and surface area to change. Based on such cell volume changes, the cell turgor pressure varies since it has to be counterbalanced by the cell wall tension. The changes in cell turgor pressure leads to the cell fluid mass gains or losses, which is governed by a mass transfer equation in the cell fluid model [14, 15]. This is repeated as a cycle until the cell

reaches a steady state condition where the cell size and the physical properties tend to reach steady values. For each cell type, this whole process was implemented and simulations were conducted.

Table 2. Values of the physical parameters adopted in the model

Parameter	Value	Reference
Initial cell fluid mass	1.767×10^{-9} kg	[14]
Initial cell wall mass	1.767×10^{-10} kg	[14]
Wall damping ratio (γ)	5×10^{-6} $Nm^{-1}s$	[14]
Cell fluid viscosity (μ)	0.1 Pas	[25]
Cell wall permeability (L_P)	2.5×10^{-6} $m^2N^{-1}s$	[28]
Fluid compression modulus (K)	20 MPa	[14]

The model was developed as a C++ source code and it was executed in a High Performance Computer (HPC). Algorithms in an existing SPH source code based on FORTRAN [18] were referred in developing the C++ source code. For the visualisations, Open Visualization Tool (OVITO) [29] was used [21]

Results and Discussion

Experimental data on drying of plant cellular materials indicate that there is an acceptable linear relationship between the removed moisture content and the bulk volumetric shrinkage [4, 30-33]. Further, the reductions of the cell area, diameter and perimeter are proportional to the overall volumetric shrinkage as well as the removed moisture content [3, 5]. All these experimental findings indicate that there is a strong connection between the moisture content of a plant food material and its shrinkage characteristics. In Figure 4, the model predictions have been visualized for apple, carrot and grape cells. Next, in order to quantify shrinkage characteristics of the cells, a set of geometrical parameters were used. Here, the moisture content (X) of the cell at a given dryness state is a critical parameter and the normalized moisture content (X/X_0) was used here to assist comparison of the model behavior over different dryness states (see Eq. 3). Similarly, the geometrical parameters used to quantify the cellular shrinkage characteristics were also normalized (see Eq. 4, 5 and 6) [14, 15]. The model predictions for these parameters were then compared with the corresponding experimental results in literature [3]. In Figure 5, normalized cell area variation for apple cells are presented and in Figure 6 and 7, normalized cell diameter variation and the normalized cell perimeter variation are presented, respectively. The parameter variation

comparison for the other types of food categories (i.e. carrot and grape) follow a similar trend and were not included here.

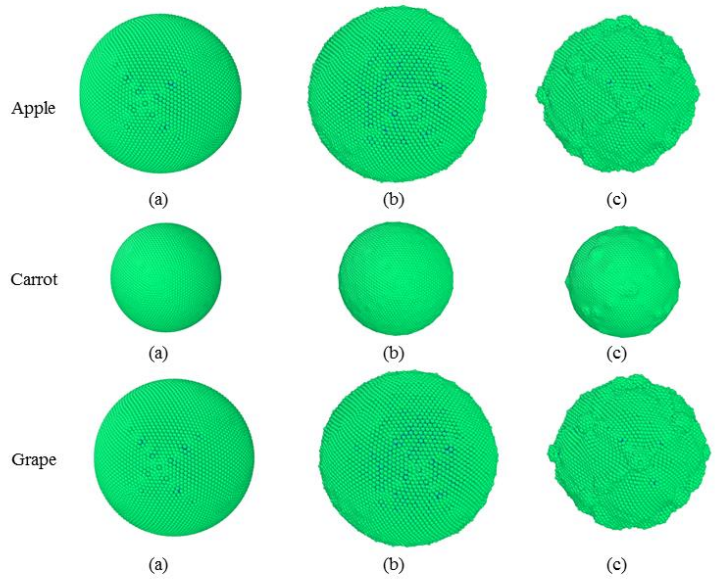

Figure 4. Visualization of the numerical results of the 3-D SPH-DEM model (a) initial conditions before simulations (b) the inflated fresh apple cell ($X/X_0 = 1$) (c) dried state ($X/X_0 = 0.1$)

In the course of this study, results of our work (see the comparisons in the Figures 5, 6 and 7) has shown that there is the possibility to successfully develop a 3-D numerical model for the simulation of single parenchyma cells of apple, carrot and grape during the process of drying using a meshfree approach. There is a reasonably good agreement between the SPH-DEM model predictions and the experimental results [3, 5]. As it could be observed in Figures 5, 6 and 7, this agreement is more positive in the higher moisture content values (i.e. $X/X_0 \geq 0.4$). When it comes to extremely low moisture contents (i.e. $X/X_0 \leq 0.25$), the model predictions tend to deviate from the realistic values considerably.

$$normalised\ moisture\ content = \frac{X}{X_0} = \frac{steady\ state\ cell\ fluid\ mass}{fresh\ cell\ fluid\ mass}. \quad (3)$$

$$normalised\ surface\ area = \frac{A}{A_0} = \frac{steady\ state\ cell\ surface\ area}{fresh\ cell\ surface\ area}. \quad (4)$$

$$normalised\ diameter = \frac{D}{D_0} = \frac{steady\ state\ cell\ Diameter}{fresh\ cell\ Diameter}. \quad (5)$$

$$normalised\ perimeter = \frac{P}{P_0} = \frac{steady\ state\ cell\ Perimeter}{fresh\ cell\ Perimeter}. \quad (6)$$

Therefore, it could be deduced that the developed 3-D SPH-DEM plant cell model has got the ability to approximate the true cellular scale drying behavior much quantitatively and

qualitatively. When comparing with the most recent 2-D numerical models for plant tissue drying [34, 35], it could be seen that this model shows great competency and potential to closely describe the true plant food tissue drying scenario, particularly in 3-D. Therefore credentials are there in these modelling schemes to be further developed and utilized in the field of food engineering. Furthermore, it should be emphasized that there is room for further improvements in the model especially at extremely dried stages ($X/X_0 \leq 0.25$). These improvements would add more details into the true deforming behavior of the cellular system.

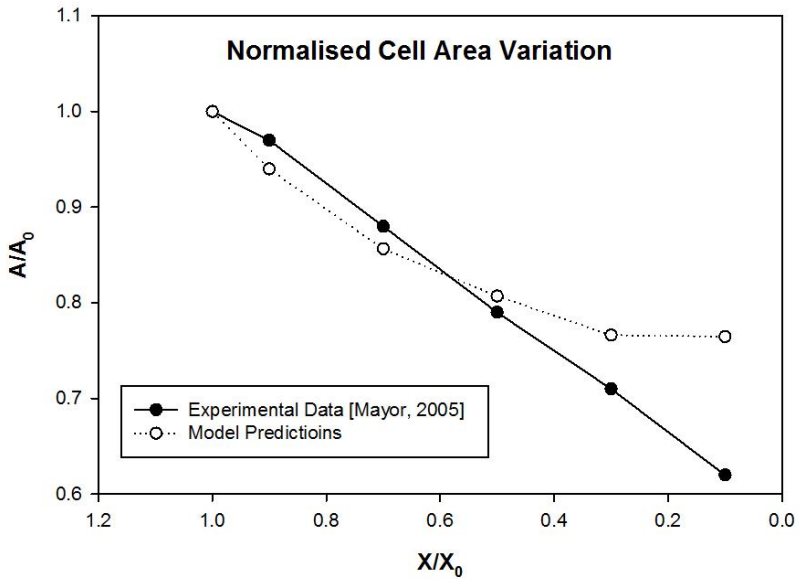

Figure 5. Comparison of model predictions and experimental results [3] for normalised cell area of a single apple cell during drying

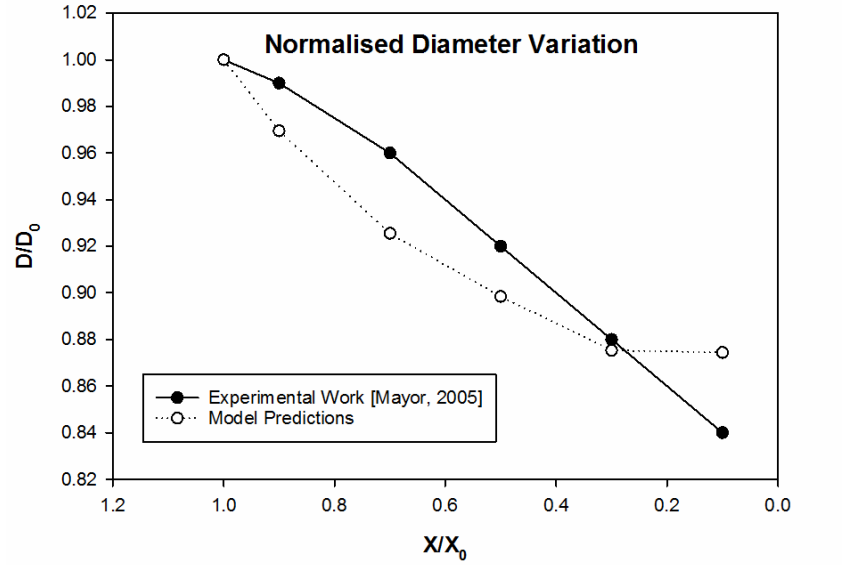

Figure 6. Comparison of model predictions and experimental results [3] for normalised cell diameter of a single apple cell during drying

Conclusion and Outlook

A 3-D plant cell model has been developed using a coupled SPH-DEM numerical method in order to predict the shrinkage characteristics during drying. The model composed of two major parts: cell fluid model and cell wall model. The cell fluid model is based on SPH and approximates the cell protoplasm to a homogeneous Newtonian liquid. The cell wall model is based on a DEM and approximates the real cell wall to an incompressible Neo-Hookean solid material. The drying of single cells of apple, carrot and grape were modelled and simulated for the drying related deformations. Cell shape parameters such as surface area, diameter and perimeter were used to quantify the cell shape alterations. The quantitative shrinkage characteristics were compared with the results from relevant experiments on similar type of plant food materials. Comparisons show that there are similar trends in experimental results and the model predictions, even though there are deviations particularly at very low moisture contents values (extremely dried states of the cells). The reasoning behind such differences have been discussed.

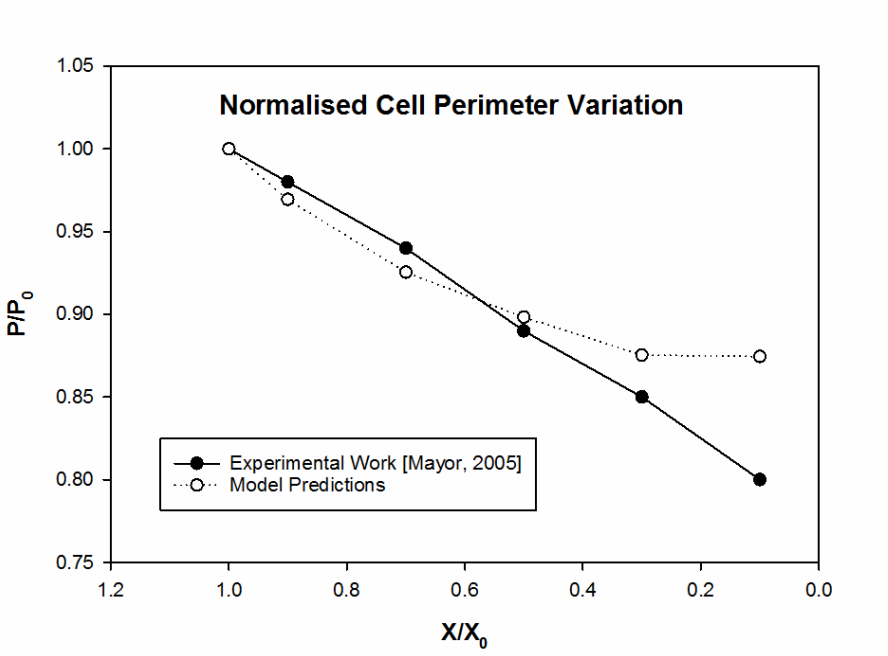

Figure 7. Comparison of model predictions and experimental results [3] for normalised cell perimeter of a single apple cell during drying

It could be noticed that the fundamental capabilities of the adopted numerical modelling technique can effectively handle large deformations of a multiphase cellular system in a comprehensive manner, particularly addressing the 3-D details. Moreover, it has been discussed that there is room for improvements, which can make the model predictions more realistic. This study has the potential to be extended to the level of multi-cell systems by using the developed single cell 3-D model as a fundamental building block.

Acknowledgements

The authors of this study kindly acknowledge the High Performance Computing (HPC) facilities of Queensland University of Technology (QUT), Brisbane, Queensland, Australia; the financial support provided by the Chemistry, Physics and Mechanical Engineering (CPME) scholarship provided by the Science and Engineering Faculty (SEF), QUT; and the

first author specifically extends the sincere support provided by University of Moratuwa, Sri Lanka.

References

1. Jangam, S.V., *An overview of recent developments and some R&D challenges related to drying of foods.* Drying Technology, 2011. **29**(12): p. 1343-1357.
2. Stefan, G., S.R. Hosahalli, and M. Michele, *Drying of Fruits, Vegetables, and Spices*, in *Handbook of Postharvest Technology*. 2003, CRC Press. p. 653-695.
3. Mayor, L., M. Silva, and A. Sereno, *Microstructural changes during drying of apple slices.* Drying technology, 2005. **23**(9-11): p. 2261-2276.
4. Lozano, J.E., E. Rotstein, and M.J. Urbicain, *TOTAL POROSITY AND OPEN-PORE POROSITY IN THE DRYING OF FRUITS.* Journal of Food Science, 1980. **45**(5): p. 1403-1407.
5. Ramos, I.N., et al., *Quantification of microstructural changes during first stage air drying of grape tissue.* Journal of Food Engineering, 2004. **62**(2): p. 159-164.
6. Hills, B.P. and B. Remigereau, *NMR studies of changes in subcellular water compartmentation in parenchyma apple tissue during drying and freezing.* International journal of food science & technology, 1997. **32**(1): p. 51-61.
7. Lee, C.Y., D.K. Salunkhe, and F.S. Nury, *Some chemical and histological changes in dehydrated apple.* Journal of the Science of Food and Agriculture, 1967. **18**(3): p. 89-93.
8. Lewicki, P.P. and G. Pawlak, *Effect of Drying on Microstructure of Plant Tissue.* Drying Technology, 2003. **21**(4): p. 657-683.
9. Ratti, C., *Hot air and freeze-drying of high-value foods: a review.* Journal of food engineering, 2001. **49**(4): p. 311-319.
10. Bartlett, M.K., C. Scoffoni, and L. Sack, *The determinants of leaf turgor loss point and prediction of drought tolerance of species and biomes: a global meta-analysis.* Ecology Letters, 2012. **15**(5): p. 393-405.
11. Crapiste, G.H., S. Whitaker, and E. Rotstein, *Drying of cellular material—I. A mass transfer theory.* Chemical Engineering Science, 1988. **43**(11): p. 2919-2928.
12. Zogzas, N., Z. Maroulis, and D. Marinos-Kouris, *Densities, shrinkage and porosity of some vegetables during air drying.* Drying Technology, 1994. **12**(7): p. 1653-1666.
13. Karathanos, V., G. Villalobos, and G. Saravacos, *Comparison of two methods of estimation of the effective moisture diffusivity from drying data.* Journal of Food Science, 1990. **55**(1): p. 218-223.
14. Karunasena, H.C.P., et al., *A coupled SPH-DEM model for micro-scale structural deformations of plant cells during drying.* Applied Mathematical Modelling, 2014. **38**(15–16): p. 3781-3801.
15. Karunasena, H.C.P., et al., *A particle based model to simulate microscale morphological changes of plant tissues during drying.* Soft Matter, 2014.
16. Karunasena, H.C.P., et al., *Numerical investigation of plant tissue porosity and its influence on cellular level shrinkage during drying.* Biosystems Engineering, 2015. **132**(0): p. 71-87.
17. Nilsson, S.B., C.H. Hertz, and S. Falk, *On the Relation between Turgor Pressure and Tissue Rigidity. II.* Physiologia Plantarum, 1958. **11**(4): p. 818-837.
18. Liu, G.-R. and M. Liu, *Smoothed particle hydrodynamics: a meshfree particle method*. 2003: World Scientific.
19. Van Liedekerke, P., et al., *Particle-based model to simulate the micromechanics of biological cells.* Physical Review E, 2010. **81**(6): p. 061906.
20. Van Liedekerke, P., et al., *A particle-based model to simulate the micromechanics of single-plant parenchyma cells and aggregates.* Physical biology, 2010. **7**(2): p. 026006.
21. Karunasena, H.C.P., et al., *Application of meshfree methods to numerically simulate microscale deformations of different plant food materials during drying.* Journal of Food Engineering, 2015. **146**(0): p. 209-226.
22. Karunasena, H.C.P., et al., *A particle based model to simulate microscale morphological changes of plant tissues during drying.* Soft Matter, 2014. **10**(29): p. 5249-5268.
23. Liedekerke, P.V., et al., *A particle based model to simulate plant cells dynamics*, in *4th international SPHERIC workshop*. 2009: Nantes, France.
24. Liedekerke, P.V., et al., *A particle-based model to simulate the micromechanics of single-plant parenchyma cells and aggregates.* Physical Biology, 2010. **7**(2): p. 026006.

25. Van Liedekerke, P., et al., *Mechanisms of soft cellular tissue bruising. A particle based simulation approach.* Soft Matter, 2011. **7**(7): p. 3580-3591.
26. Karunasena, H.C.P., et al., *Simulation of plant cell shrinkage during drying – A SPH–DEM approach.* Engineering Analysis with Boundary Elements, 2014. **44**(0): p. 1-18.
27. Helambage, C.P.K., et al., *A meshfree model for plant tissue deformations during drying.* ANZIAM Journal, 2014. **55**: p. C110-C137.
28. Taiz, L. and E. Zeiger, *Plant physiology.* New York: Sinauer, 2002.
29. Alexander, S., *Visualization and analysis of atomistic simulation data with OVITO–the Open Visualization Tool.* Modelling and Simulation in Materials Science and Engineering, 2010. **18**(1): p. 015012.
30. Moreira, R., A. Figueiredo, and A. Sereno, *Shrinkage of apple disks during drying by warm air convection and freeze drying.* Drying Technology, 2000. **18**(1-2): p. 279-294.
31. Mayor, L. and A.M. Sereno, *Modelling shrinkage during convective drying of food materials: a review.* Journal of Food Engineering, 2004. **61**(3): p. 373-386.
32. Ratti, C., *Shrinkage during drying of foodstuffs.* Journal of Food Engineering, 1994. **23**(1): p. 91-105.
33. SUZUKI, K., et al., *Shrinkage in dehydration of root vegetables.* Journal of Food Science, 1976. **41**(5): p. 1189-1193.
34. Karunasena, H., et al., *Numerical Investigation of Case Hardening of Plant Tissue During Drying and Its Influence on the Cellular-Level Shrinkage.* Drying Technology, 2015. **33**(6): p. 713-734.
35. Fanta, S.W., et al., *Microscale modeling of coupled water transport and mechanical deformation of fruit tissue during dehydration.* Journal of Food Engineering, 2014. **124**: p. 86-96.